ACADEMIC PRESS

Available online at www.sciencedirect.com

SCIENCE DIRECT®

Analytical Biochemistry 317 (2003) 218–225

ANALYTICAL BIOCHEMISTRY

www.elsevier.com/locate/yabio

Validation of an algorithm for automatic quantification of nucleic acid copy numbers by real-time polymerase chain reaction

Jochen Wilhelm,* Alfred Pingoud, and Meinhard Hahn[1]

Institut für Biochemie, FB 08, Justus-Liebig-Universität Giessen, Heinrich-Buff-Ring 58, D-35392 Giessen, Germany

Received 3 December 2002

Abstract

Real-time quantitative polymerase chain reaction (PCR) with on-line fluorescence detection has become an important technique not only for determination of the absolute or relative copy number of nucleic acids but also for mutation detection, which is usually done by measuring melting curves. Optimum assay conditions have been established for a variety of targets and experimental setups, but only limited attention has been directed to data evaluation and validation of the results. In this work, algorithms for the processing of real-time PCR data are evaluated for several target sequences (*p53*, *IGF-1*, *PAI-1*, *Factor VIIc*) and compared to the results obtained by standard procedures. The algorithms are implemented in software called *So*FAR, which allows fully automatic analysis of real-time PCR data obtained with a Roche LightCycler instrument. The software yields results with considerably increased precision and accuracy of quantifications. This is achieved mainly by the correction of amplification-independent signal trends and a robust fit of the exponential phase of the signal curves. The melting curve data are corrected for signal changes not due to the melting process and are smoothed by fitting cubic splines. Therefore, sensitivity, resolution, and accuracy of melting curve analyses are improved.

Keywords: Quantitative real-time PCR; LightCycler; Algorithm; Fluorescence resonance energy transfer; Hybridization probes

The polymerase chain reaction (PCR) is a frequently used technique to determine the concentration of a specific target sequence within samples of nucleic acids. The sequences of interest are exponentially amplified from template molecules by an in vitro DNA replication process to obtain dsDNA products that can be further analyzed. In conventional endpoint analyses, the amount of PCR products at the end of the amplification reaction is used to estimate the amount of template molecules. The detection of the products can be done by densitometric analysis of gels stained with ethidium bromide [1] or SYBR GreenI [2] or by detection of incorporated radioactive [3] or fluorescent [4] probes.

Where the amplification is not limited by any reaction component, the concentration of the PCR product is exclusively proportional to the template concentration, i.e., the product concentrations can be used to estimate the template concentration only when the amplification reaction has not reached the plateau phase of product accumulation. This limitation is circumvented by quantitative competitive PCR (QC-PCR)[2] [5] which relies on the constancy of the ratio between target and competitor products during the amplification, including the plateau phase. Although QC-PCR is known to be one of the most exact methods for the quantification of nucleic acids, it is laborious (generation of ideal competitors, discrimination of PCR products specific for target and competitor, titrating the equivalence point) and requires relatively large amounts of target DNA.

More sophisticated, real-time PCR assays measure the product accumulation during the amplification

* Corresponding author. Fax: +49-641-9935409.
E-mail address: Jochen.Wilhelm@chemie.bio.uni-giessen.de (J. Wilhelm).
[1] Present address: Abteilung Molekulare Genetik, B060, Deutsches Krebsforschungszentrum Im Neuenheimer Feld 280, D-69120 Heidelberg, Germany.

[2] *Abbreviation used*: QC-PCR, quantitative competitive PCR.

0003-2697/03/$ - see front matter © 2003 Elsevier Science (USA). All rights reserved.
doi:10.1016/S0003-2697(03)00167-2

reaction by determining the fluorescence emission of probes, which is being proportional to the amount of PCR product [6–8]. The major advantages of this technique are the high dynamic range of quantification and the avoidance of laborious post-PCR analytical steps with the risk of carryover contamination by PCR products. The signal generation can be achieved either by dsDNA-specific fluorescent dyes such as SYBR Green I [8,9] or by fluorescence resonance energy transfer or quench reduction of fluorophor-labeled oligonucleotides as sequence-specific probes [7,10–15]. Once the time course of product accumulation for the complete reaction is known, the efficiency of the amplification can be calculated. Then, the template concentration can be derived from the number of amplification cycles (C_T) needed to generate a certain product concentration, i.e., when the fluorescence signal reaches a threshold value. Usually, the determination of the efficiency is done by the evaluation of C_T values of a dilution series of a standard sample. If the template concentration of the standard is known, this information can be used for absolute quantifications: the C_T values of a standard dilution series plotted versus the logarithm of their known initial concentrations are ideally on a straight line. The regression line through these points is used to determine the amplification efficiency and to quantify the unknown template concentrations in the samples by their C_T values. Obviously, this exponential proportionality is valid only if the threshold value is within the exponential part of *all* signal curves used.

The correct determination of the C_T values is a crucial point in the field of real-time quantitative PCR. It relies on the identification of the exponential phases of the signal curves and the accurate calculation of the point of intersection of the threshold line and the signal curve, i.e., the C_T value, for which the points of the signal curves have to be interpolated. In practice, this technique has several pitfalls: (i) Only few data points are used for interpolation. Therefore, the interpolation and thus the C_T value is strongly influenced by signal noise. (ii) The individual signal curves can exhibit different offsets (i.e., they start with different absolute fluorescence intensities) and amplification-independent trends, which might not allow use of the same threshold value for all samples. The software usually corrects the different initial signal offsets of each signal curve by subtraction of a signal value obtained from the first data points (''initial value subtraction'') or from the data points with the lowest fluorescence intensity (''minimum value subtraction''), as is done by the LightCycler software. (iii) Nonlinear, amplification-independent signal trends, due to changes in buffer conditions during PCR or due to excimer formation of the fluorophors, are not corrected. Therefore, the exponential accumulation of the product is not directly represented by the exponential segment of the signal curves.

To calculate the C_T value of a sample, an arbitrary noise band (or threshold) has to be defined (''noise band method''). It should be placed as low as possible, but higher than the signal noise. In the next step, two to four points of the log signal values, which are higher than the noise band, are interpolated by linear regression. The C_T value is defined as the fractional cycle number where the regression line intersects the noise band. Because only few points are used for the regression analysis, this is very susceptible to errors due to noise. In addition, the exponential range is not well defined. Therefore, points of the signal course which are not within the exponential phase are sometimes used for evaluation. Finally, there are no objective guidelines given for valid noise band values. The line must cross all amplification curves of the standards and the samples to be quantified at the onset of their exponential phase. When the noise band is set too low or too high, the results are influenced by noise or by the plateau phase, respectively.

Here, we validate previously described algorithms [16] for the reliable and automatic evaluation of amplification curves obtained with the Roche LightCycler instrument and demonstrate the gain in precision and accuracy compared to the standard ''fit-points'' method. The evaluation was done using several target sequences (*p53*, *IGF-1*, *PAI-1*, *FVIIc*). All target sequences analyzed showed comparable results. Representative data are provided.

Materials and methods

DNA isolation, primer and probe sequences, PCR conditions, and melting curve sampling have been described earlier ([17] (*p53*, *IGF-1*), [18] (*PAI-1*, *FVIIc*)).

The algorithms used for data evaluation are described elsewhere [16]. They are implemented in software which can read the data files created by the LightCycler instrument. The results obtained from the evaluation of the data with the ''conventional'' procedure and with the new algorithms were compared. The conventional fit-points method includes the subtraction of the minimum value of each signal curve, whereas the new method additionally corrects the individual curves for amplification-independent trends, automatically detects the observable exponential phase, and fits it by a sigmoidal function. The new algorithm uses this function to directly calculate the C_T value for any given threshold value (''threshold method''). The optimum threshold value is determined from the error of the resulting calibration curve.

Amplification-independent trends of amplification curves were corrected using the background function described in [16],

$$B(x) = a \cdot (1 - e^{-bx}) + c,$$

where x is the cycle number, a is the saturation value; b is the slope parameter, and c is the signal-offset. The parameters a, b, and c were determined automatically by a least-squares fit of the signal curve, using the points before the exponential phase. The distribution of the residuals was analyzed to validate the suitability of the function for describing the trends. The suitability of the normal distribution for describing the observed distribution was estimated by a regression analysis of the cumulative data.

The signal curves were analyzed using all available combinations of settings for background correction (minimum subtraction or trend correction), interpolating functions (see below) and C_T calculation method (noise band or threshold).

For the threshold method, three different types of functions were tested:

$$\text{Growth function:} \quad A(x) = N_0 \cdot e^{r \cdot x}, \tag{1}$$

$$\text{Logistic function:} \quad A(x) = N_{max} \cdot \frac{x^r}{x^r + x_T^r}, \tag{2}$$

Sigmoidal exponential function:

$$A(x) = N_{max} \cdot \frac{1}{1 + e^{-r \cdot (x_T - x)}}. \tag{3}$$

The variable x denotes the amplification cycle. The parameter N_0 corresponds to the amount of template, N_{max} is the plateau value, r is the efficiency parameter of the amplification, and x_T is the cycle of the turning point of the curve. The parameter r is related to the amplification efficiency but does not describe it directly. In Eq. (1), r is simply the ln of the efficiency, in Eqs. (2) and (3), the relationship between r and the efficiency is more indirect with r adjusting the slope of the function in the turning point ($x = x_T$). To compare the applicability of these functions, C_T values for sets of identical PCRs were calculated and the standard deviations of the C_T values obtained were determined. Additionally, the tolerance for noise was tested similarly on a median curve calculated for 32 replicates where Gaussian noise was added. The median curve was obtained from the median, i.e., the value in the middle of the sorted row of the 32 data points, at each cycle. As template DNA, a *p53* PCR product [17] which was reamplified in 32 replicates was used. The Gaussian noise was generated using the Box–Muller method [19]. Standard deviations of the C_T values were calculated for sets of 50 curves with added noise.

If standard dilution series were measured, the noise band or threshold was chosen to minimize the error of the calibration curve. In analyses without standards, either the threshold value was set in the middle of the exponential phase (for the threshold method) or the noise band value was set to the lower limit of the exponential phase (for the noise band method). Therefore, for both methods the points in the middle of the exponential phase of the signal curves were used for the determination of the C_T values.

Results

Signal curves from the amplification of all target sequences (*p53*, *IGF-1*, *PAI-1*, *FVIIc*) were analyzed. The signal curves showed different efficiencies, signal yields, and signal-to-noise ratios. The analysis results were qualitatively similar for all target sequences. The increase in precision of the quantification using the new algorithms was greater for signal curves with a lower signal-to-noise ratio. Improvements of accuracy were greater for signal curves with more pronounced amplification-independent signal trends. Here, representative data are shown to demonstrate the diverse effects.

Validation of the correction of background trends in amplification curves

The effect of the background correction of real-time PCR amplification curves is shown in Fig. 1. The amplification-independent signal trends are reliably identified within a template concentration range spanning eight orders of magnitude. The applicability of the saturation function $(B(x))$ as background function is demonstrated by the analysis of the distribution of $(y_i - B(x_i))$ within the data range used for the least squares fit of B. The fit of a normal distribution function to the determined distribution reveals a standard deviation of 2.04×10^{-4} for the signal ratio (Ch. 2/1, $R^2 = 0.9981$) and 4.86×10^{-3} for the acceptor signal only (Ch. 2, $R^2 = 0.9630$) (data not shown). The relative noise (i.e., the standard deviation divided by the maximum plateau signal) is similar in both cases (0.6 and 0.7%, respectively).

After background correction, the slopes of the log-linear segments of the signal curves are altered (see Figs. 1b and d). The amplification efficiencies calculated from the slopes of the curves still including background trends decrease with decreasing template concentration. After correction of the trends, the calculated efficiencies are approximately constant and do not show such a concentration dependence (Fig. 2a). The concentration dependence of the slopes has an influence on the efficiency calculated using the slope of the standard curve. Without correction, the efficiency determined decreases with increasing threshold values. After correction, the dependency on the threshold value is almost completely eliminated (Fig. 2b).

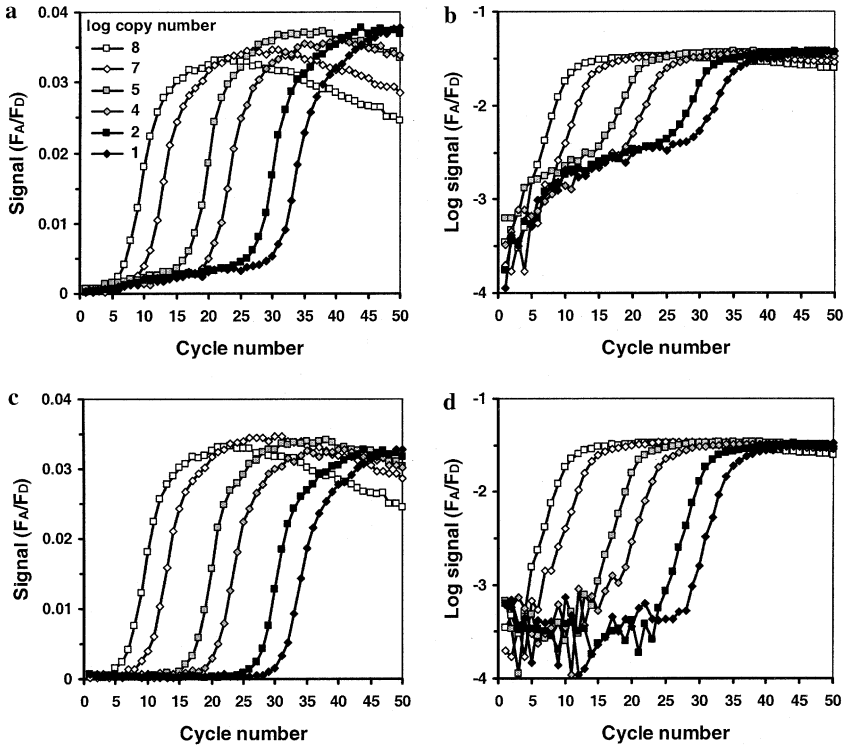

Fig. 1. Effect of background correction on signal curves. (a) Signal curves of a standard dilution series. The template was a 125-bp *IGF-1*-specific PCR product. Amplification was carried out with the same primers; the product was detected with the *IGF-1*-specific hybridization probes. (b) Half-logarithmic representation of the data shown in (a). (c) Same data as show in (a) after background correction. (d) Half-logarithmic representation of the data shown in (c).

Comparison of amplification functions

Three different amplification functions (Eqs. (1)–(3)), see Materials and methods) were tested for their applicability by testing the precision of the C_T values determined on data sets with different noise levels (data not shown). For noise with a standard deviation of less than 0.5% of the plateau signal value, the growth function (Eq. (1)) was 10 to 15% more precise than the logistic function (Eq. (2)). For higher noise levels, it was the opposite way around. In all cases, the sigmoidal exponential function (Eq. (3)) was 10 to 25% more precise than both other functions tested. Therefore, the sigmoidal exponential function was used for all subsequent analyses.

Precision and relative insensitivity toward noise

The influences of the background correction and the C_T calculation method on precision were investigated using data from 5-fold replicates and 32-fold replicates (Fig. 3). The standard deviation of the C_T values determined for identical replicates is an indicator of precision. The standard deviations obtained for the uncorrected data are always higher than those for the corrected data. The determination of the C_T values obtained with the threshold method was always more precise than that with the noiseband method. In addition, the use of the signal ratio (Ch. 2/1) always resulted in lower standard deviations. In general, the combination of Ch. 2/1, background correction, and threshold method yielded the most precise results.

The robustness of the C_T calculation methods toward noise was analyzed on a median data curve which was overlaid with increasing Gaussian noise (data not shown). The standard deviations of the C_T values determined from sets of 50 repeated calculations increased linearly with the noise factor. The threshold method yields approximately 20% more precise results than the noiseband method, independent of the amount of noise added.

Accuracy

Examples of the gains in accuracy and precision when the developed algorithms are applied are shown in Fig. 4. The test sample is a defined dilution of the standard DNA stock solution, containing 800 template copies. The standard procedure for evaluation yielded 544 ± 379 copies (mean $\pm$ SD) for the test sample. The same data, background corrected and analyzed with the threshold method, yielded 813 ± 115 copies (mean $\pm$ SD). Both threshold and noise band values were chosen for a minimum error of the resulting standard curve.

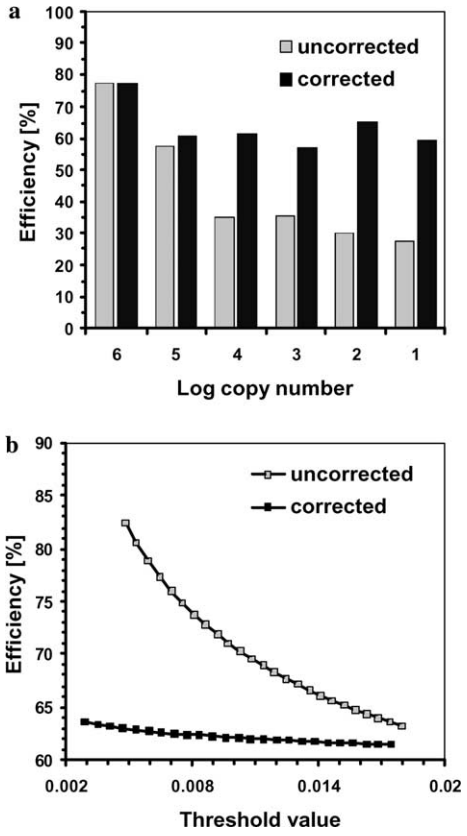

Fig. 2. Effect of background correction on efficiency calculations. The template was an *IGF-1*-specific PCR product of 125 bp. Amplification was carried out with the same primers; the product was detected with the *IGF-1* hybridization probes. (a) Efficiencies determined from individual signal curves of samples with different template copy numbers. The efficiencies were derived from the growth function fitted to the exponential phases of each curve. (b) Efficiencies determined from the slope of the calibration curve depending on the threshold value (threshold value range = common range of exponential phases of all standards).

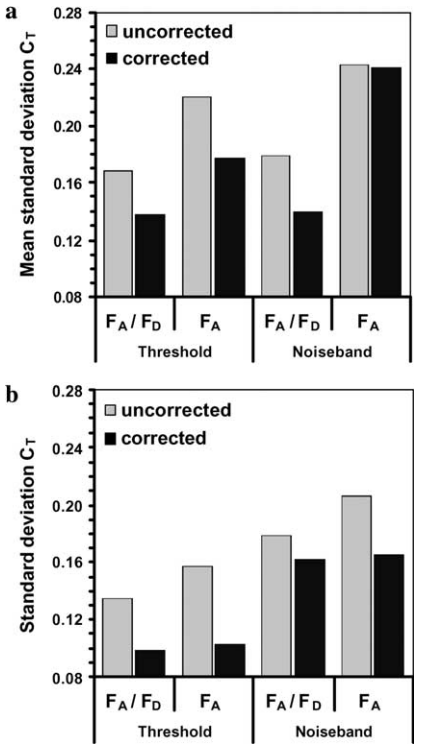

Fig. 3. Precision of C_T calculations. Human genomic DNA was amplified with primers specific for the human *p53* gene; the 125-bp PCR product was detected with the *p53*-specific hybridization probes. C_T values of the samples were calculated using the data of channel 2/1 (F_A/F_D) or of channel 2 (F_A) and the threshold method or noiseband method (with three fit points). (a) Mean standard deviations of C_T values ($n = 125$:5 different samples × 5 replicates × 5 different runs). Each run contained a standard dilution series. The threshold and noiseband values were adjusted to minimize the standard error of the calibration curve. Standard deviations of the C_T values were determined per group of five identical experiments. (b) Standard deviations of the C_T values of 32 identical experiments. The threshold value was set in the middle of the exponential phase; the noiseband value was set to the lower limit of the exponential phase.

The experiments used the same source of DNA (i.e., a stock solution of human genomic DNA) for both standards and samples. To determine the accuracy, it is therefore not necessary to know the "true" template concentration in the sample.

Discussion

In the life sciences, increasingly more experimental data are acquired and processed electronically. The fast development of new techniques for automated and high-throughput methods requires powerful software not only for the data acquisition but also for the evaluation of the data. It is counterproductive if the large amounts of automatically acquired data still have to be screened, selected, and evaluated manually. Additionally, often not all available data are used for evaluation, because the evaluation methods used, although operating electronically, were not adapted to the potential of modern computers. This situation occurs also given in the case of real-time PCR techniques.

In one of the first publications dealing with quantitative real-time PCR, Higuchi et al. [6] demonstrated the linear relationship between the C_T values and the log of the starting copy number for an arbitrarily chosen threshold value. Later, this was shown again by Heid et al. [7] who first suggested a procedure to obtain a more objectively defined threshold value, namely to take 10 times the standard deviation of the fluorescence signals of the first 3 to 10 amplification cycles (ABI7700 tutorial). As can be seen in Fig. 3a, this method would not yield satisfactory results on data with signal trends in the first cycles. Those authors neither explained the method of C_T determination nor investigated the influence of signal noise on the precision of the calculated C_T values. Wittwer et al. [20] fitted the exponential growth

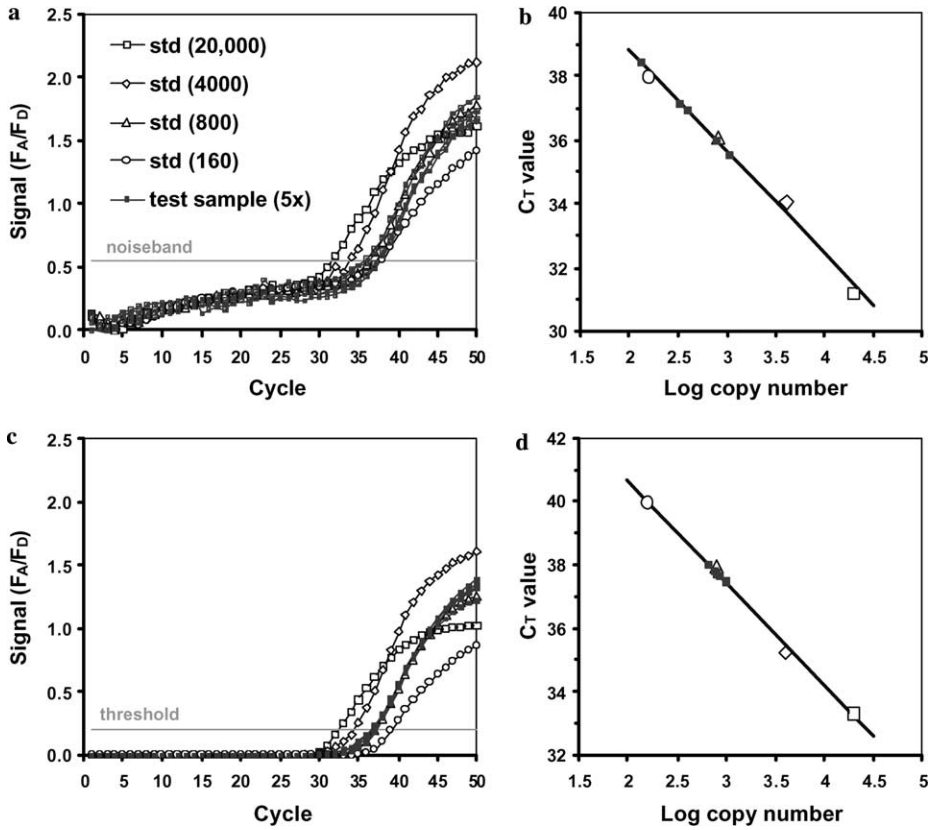

Fig. 4. Accuracy of quantifications with noisy data. Human genomic DNA was amplified with the *p53*-specific primers; the 125-bp PCR product was detected with the p53-specific hybridization probes. C_T values of the samples were calculated using the data of channel 2/1. (a) Kinetic PCR data of a standard dilution series and test sample measured in five identical experiments without background correction. The noiseband value for quantification is indicated by the horizontal line. The test samples were pipetted from the same stock solution and contained 800 copies of genomic DNA. (b) Calibration curve of the data shown in (a). The C_T values were determined with the noiseband method (three fit points per curve). The C_T values of the test samples are projected on the line. (c) Same data as shown in (a), after background correction. (d) Calibration curve of the background-corrected data.

function to the exponential phase of the signal curves or, more precisely, a regression line to the log signal curves to determine the C_T values. This method is known today as the fit-points method. The possible usefulness of a sigmoidal function for a better approximation of the signal data had been discussed [20]. However, until today the suitability of sigmoidal functions for fitting real-time PCR data has only been shown in simulations [21]. Instead, the latest Roche LightCycler software, Version 3, introduced a new method for the calculation of C_T values, the second derivative maximum method. The advantage is the invariance to scale and offsets, but the applicability of this method still is questionable: the linear relationship between the log starting copy number and the C_T value is given only for C_T values determined during the exponential phase of the reaction. Here, the second derivative ideally is constant. The existence of a maximum in the second derivative of a signal curve is due to (i) the fact that, at the beginning of the PCR, accumulating product cannot be detected and (ii) the influence of factors limiting amplification at the onset of the plateau phase, the characteristics of which are influenced by stochastic effects. As a result, the C_T values determined by this method may be sensitive to minor variances of the signal curve characteristics and to stochastic effects of the plateau phase. Another possible pitfall here is the strong influence of noise on the determination of the derivatives and signal curves with unusual trends during the late cycles.

However, the observable exponential phase remains the only legitimate part of the signal curve that may be used for the determination of C_T values. The available software programs do not identify these sections automatically. The user has either to rely on the validity of the threshold set using the signal noise or to determine the start of the exponential phases by defining a noiseband value that clearly crosses all sample curves in the lower part of the log-linear phase as shown in a plot of log signal versus cycle number (see ABI7700 tutorial and the Roche LightCycler Operator's Manual). In any case, a prerequisite for the correct identification of exponential or log-linear phases is the correction of the background signal (positive or negative) that is supposed to add to the amplification signal: an exponential function

with any term added will not appear as a linear segment in a half-logarithmic plot. In the case of an added positive constant, the observed log-linear phase will be shifted toward the plateau phase and, therefore, will not represent the underlying exponential product accumulation. This problem can easily be circumvented by subtracting the individual offsets, provided that they are cycle independent. This procedure is still not able to correct amplification-independent trends that will mask the exponential phases and therefore cause inaccuracies (Figs. 1a and b).

The algorithm described in this work solves all these problems and allows the automatic detection of the observable exponential phases. The reasonability of the adaptive background correction compared to the simple subtraction of constant offset values is attested by the increased homogeneity of efficiencies derived from the individual signal curves within a run and the increased precision and accuracy obtained, although the reasons for the amplification-independent trends are still not clear. These trends occur in both the acceptor fluorophor signal and the donor fluorophor signal; they also occur in the absence of template and in the absence of polymerase. The shapes of these trends depend on the buffer conditions, the cycling protocol, and the sequence of the probes (data not shown). The background function $B(x)$ used in this work was well suited to describe the shape of these trends. This is confirmed by the normally distributed deviations of the signal values from the calculated values of the fitted function $B(x)$. If the function $B(x)$ was not suited to describe the amplification-independent trends correctly, the corrected values would systematically deviate from zero, resulting in a obvious nonsymmetric distribution curve.

For quantifications by real-time PCR, the amplification efficiencies of all samples used must be equal, i.e., the exponential phases of the signal curves must be parallel. Otherwise, the described relationship between the C_T values and the template copy number ($C_T = m \cdot (\log N_0) + b$, see Materials and methods) is not valid. In practice, especially for hybridization probes, the observed exponential phases which are used for the determination of the C_T values are not parallel (Fig. 1b), yielding a systematic error of the calibration curve derived. Here, we show that this error is due to amplification independent signal trends. The correction of these trends yields signal curves with parallel exponential phases (Fig. 1d). Notably, the calculated amplification efficiencies from the corrected individual signal curves are significantly more similar to the amplification efficiency calculated from the calibration curve, which no longer depends on the threshold value (Fig. 2). This supports the assumption that the correction of the signal curves removes exclusively the amplification-independent signal changes and practically isolates the underlying amplification process.

The correction of amplification-independent signal trends improves the precision of quantifications, independent of the method of C_T value determination, the data used for amplification curves, and the method of choosing the threshold (Fig. 3). The highest precisions are achieved with the acceptor-to-donor ratio of the fluorescence signals as shown earlier for different primer/probe systems [17]. In this case, stochastic effects which contribute similarly to any kind of fluorescence signal and, therefore, alter donor and acceptor fluorescence similarly, e.g., small deviations in positioning of the capillaries, are eliminated. Systematic effects with a greater influence on either of the fluorophors may alter amplification-independent trends in the amplification curves which are corrected by the algorithm described.

With signal curves with a high signal-to-noise ratio, the influence of the method of determination of C_T values on the precision is negligible. The small difference of the mean standard deviations derived from the corrected F_A/F_D amplification curves for "Threshold" and "Noiseband" (fit-points method) in Fig. 3 may be due to the high signal-to-noise ratio of the raw data used. For noisy data, the threshold method yields more precise results. This is indicated by larger differences in the mean standard deviations derived from the acceptor signals F_A of the same experiments which usually are more noisy than the signal ratios F_A/F_D (Fig. 3). The signal-to-noise ratio is inversely proportional to the standard deviation of the C_T values obtained from identical experiments (data not shown). The proportionality factor is larger for the fit-points method (noiseband) than for to the threshold method, confirming that the threshold method is less sensitive to noise than the fit-points method. The linear relationship between noise and precision for the level of C_T values changes to an exponential relationship for the level of concentrations or copy numbers derived from the C_T values.

Taken together, the adaptive background trend correction and the threshold method for the determination of C_T values increase not only the precision but also the accuracy, as shown for a quantification experiment in Fig. 4 (544 ± 379 copies (mean $\pm$ SD) after conventional evaluation versus 813 ± 115 copies after evaluation using the algorithms described here). This difference in precision and accuracy cannot be estimated from the correlation coefficients of the calibration curves, which were only marginally different (0.9896 without and 0.9956 with correction). In fact, the correlation coefficient of the calibration curve gives only a poor estimate for the precision or accuracy achieved, which, therefore, should not be used to compare the quality of quantification results of different experiments.

In general, coefficients of variation of 2–10% for quantifications can be achieved reproducibly even from noisy data by real-time PCR using the SoFAR

algorithms for data evaluation [16]. This precision is similar to the one obtained by QC-PCR with internal standardization. QC-PCR has the advantage of being less sensitive to polymerase inhibitors in the samples than methods based on external standardization such as real-time PCR. QC-PCR, however, requires larger amounts of sample DNA and is more laborious and time-consuming.

Conclusions

The algorithm for the evaluation of amplification curves yields significantly more precise and accurate results than the conventionally used algorithms. It is very robust, can handle even very noisy data without human intervention, and, therefore, allows for completely automated and reliable evaluation of quantifications by real-time PCR as would be required for high-throughput assays.

Acknowledgments

This work was supported by the Deutsche Forschungsgemeinschaft (Graduiertenkolleg *Molekulare Biologie und Pharmakologie*) and the Fonds der Chemischen Industrie.

References

[1] S. Abbs, M. Bobrow, Analysis of quantitative PCR for the diagnosis of deletion and duplication carriers in the dystrophin gene, J. Med. Genet. 29 (1992) 191–196.
[2] C. Schneeberger, P. Speiser, F. Kury, R. Zeillinger, Quantitative detection of reverse transcriptase-PCR products by means of a novel and sensitive DNA stain, PCR Methods Appl. 4 (1995) 234–238.
[3] L. Pastore, M.G. Caporaso, G. Frisso, A. Orsini, L. Santoro, L. Sacchetti, F. Salvatore, A quantitative polymerase chain reaction (PCR) assay completely discriminates between Duchenne and Becker muscular dystrophy deletion carriers and normal females, Mol. Cell. Probes 10 (1996) 129–137.
[4] A. Landgraf, B. Reckmann, A. Pingoud, Quantitative analysis of polymerase chain reaction (PCR) products using primers labeled with biotin and a fluorescent dye, Anal. Biochem. 193 (1991) 231–235.
[5] K. Zimmermann, J.W. Mannhalter, Technical aspects of quantitative competitive PCR, BioTechniques 21 (1996) 268–272, 274–279.
[6] R. Higuchi, C. Fockler, G. Dollinger, R. Watson, Kinetic PCR analysis: real-time monitoring of DNA amplification reactions, Biotechnology (NY) 11 (1993) 1026–1030.
[7] C.A. Heid, J. Stevens, K.L. Livak, P.M. Williams, Real time quantitative PCR, Genome Res. 6 (1996) 986–994.
[8] C.T. Wittwer, M.G. Herrmann, A.A. Moss, R.P. Rasmussen, Continuous fluorescence monitoring of rapid cycle DNA amplification, BioTechniques 22 (1997) 130–131, 134–138.
[9] T.B. Morrison, J.J. Weis, C.T. Wittwer, Quantification of low-copy transcripts by continuous SYBR-GreenI monitoring during amplification, BioTechniques 24 (1998) 954–958, 960, 962.
[10] P.M. Holland, R.D. Abramson, R. Watson, D.H. Gelfand, Detection of specific polymerase chain reaction product by utilizing the $5' \rightarrow 3'$ exonuclease activity of *Thermus aquaticus* DNA polymerase, Proc. Natl. Acad. Sci. USA 88 (1991) 7276–7280.
[11] S. Tyagi, F.R. Kramer, Molecular beacons: probes that fluoresce upon hybridization, Nat. Biotechnol. 14 (1996) 303–308.
[12] I.A. Nazarenko, S.K. Bhatnagar, R.J. Hohman, A closed tube format for amplification and detection of DNA based on energy transfer, Nucleic Acids Res. 25 (1997) 2516–2521.
[13] L.G. Kostrikis, S. Tyagi, M.M. Mhlanga, D.D. Ho, F.R. Kramer, Spectral genotyping of human alleles, Science 279 (1998) 1228–1229.
[14] D. De Silva, C.T. Wittwer, Monitoring hybridization during polymerase chain reaction, J. Chromatogr. B Biomed. Sci. Appl. 741 (2000) 3–13.
[15] D. Whitcombe, J. Theaker, S.P. Guy, T. Brown, S. Little, Detection of PCR products using self-probing amplicons and fluorescence, Nat. Biotechnol. 17 (1999) 804–807.
[16] J. Wilhelm, A. Pingoud, M. Hahn, SoFAR: Software for fully automatic and accurate evaluation of real-time PCR data, BioTechniques 34 (2003) 324–332.
[17] J. Wilhelm, A. Pingoud, M. Hahn, Comparison between *Taq* DNA polymerase and its Stoffel fragment for quantitative real-time PCR with hybridization probes, BioTechniques 30 (2001) 1052–1056, 1058, 1060.
[18] J. Wilhelm, H. Reuter, B. Tews, A. Pingoud, M. Hahn, Detection and quantification of insertion/deletion-variations by allele-specific real-time PCR: application for genotyping and chimerism analysis, Biol. Chem. 383 (2002) 1423–1433.
[19] D.E. Knuth, The Art of Computer Programming, Vol. 2, second ed., Edison-Wesley, 1981, p. 116ff.
[20] C.T. Wittwer, K.M. Ririe, R.P. Rasmussen, Fluorescence monitoring of rapid-cycle PCR for quantification, in: F. Ferré (Ed.), Gene Quantification, Birkhäuser, Boston, 1997, pp. 129–144.
[21] W. Liu, D.A. Saint, A new quantitative method of real time reverse transcription polymerase chain reaction assay based on simulation of polymerase chain reaction kinetics, Anal. Biochem. 302 (2002) 52–59, doi:10.1006/abio.2001.5530.